Z-99 Numerical study of scattering attenuation in fractured media: frequency dependence and effects of characteristic length scales.

Serafeim Vlastos [1,2], Clement Narteau [2], Enru Liu [1] and Ian Main [2]
[1]*British Geological Survey, Murchison House, West Mains Road, Edinburgh EH9 3LA, UK*
[2]*Department of Geology and Geophysics, University of Edinburgh, UK*

Introduction

Seismic attenuation is, in general, a combined effect of absorption (intrinsic attenuation), which is affected by lithological parameters, and scattering (apparent) attenuation, which is related to structural parameters. Which of these two mechanisms dominates in any given situation depends on the relative wavelengths of the seismic wave and the heterogeneities of the fracture system. In this study, we deal exclusively with scattering attenuation. Synthetic modeling studies with and without intrinsic attenuation show that the contribution of scattering attenuation is significant. Scattering involves no energy loss, but produces a more extended, lower amplitude wavetrain by the resulting interference. It is dependent on the nature of small-scale fluctuations in the earth parameters and is found to be frequency dependent. In the study, for the numerical simulations we use a 2-D finite – difference method that can accurately model the effects of scattering in a fractured network (Vlastos et al., 2002). The various fracture patterns examined are patterns of development of a population of fractures involving nucleation, growth, branching, interaction and coalescence created by a multiscale cellular automaton model (Narteau, 2001). The main aim of this study is to examine the behaviour of scattering attenuation at different fracture patterns characterized by different statistical properties, fracture population geometry and criticality. We examine scattering attenuation in a range of frequencies for each one of the fracture patterns and demonstrate the frequency dependence. The comparison of the pattern of scattering attenuation with frequency between different fracture patterns shows that there is a change that can be attributed to the changes in the statistical properties of the fracture population. We conclude by examining the existence of direct links between the fracture properties and the scattering attenuation pattern that can be used for the characterisation of fractured reservoir.

Generation of fault patterns

Over the last ten years, the modeling of fracture populations has become a well-established approach with a large variety of applications. In this study a multiscale cellular automaton model (Narteau, 2001) generates the fracture patterns. It is a multiscale model of rupture of a crustal shear under constant external forcing and reproduces different structural properties that are observed in the formation and evolution of a population of strike-slip fractures. At the smallest scale, the dynamical system is determined by a time dependent stochastic process with two states of fracturing (active and stable). At larger scale, the state of fracturing is determined by purely geometric rules of fracture interaction based on fracture mechanics. In addition to these short range interactions, a redistribution mechanism in the neighbourhood of active fractures ensures long range interactions. Thus, non-linear feedback processes are incorporated in the fracture growth mechanism. Nucleation, growth, branching, interaction and coalescence are described as the successive expressions of a more general process of localization. In Figure 1 we show the three fracture patterns that we will examine. They are generated from the cellular automaton and they represent consecutive steps of the evolution of the fracture patterns. Figure 1a represents the early stage of the evolution of the fractures, Figure 1b represents the a stage that is after the percolation threshold, and Figure 1c is near the ending stages when we are moving towards the quasi-steady state (i.e. stable fault population over long time).

Numerical simulation

To examine the variation in scattering attenuation for the different stages of the fracture evolution and to investigate their frequency dependence, we conduct forward modeling for each model. We use a finite-difference method that can accurately model complicated fractured networks with fractures at

arbitrary angles to the grid (Vlastos et al., 2002). To ensure consistency between the different models we use the same background medium in all the cases. That will guarantee that any variation in scattering attenuation is due to the different properties of the modeled medium.

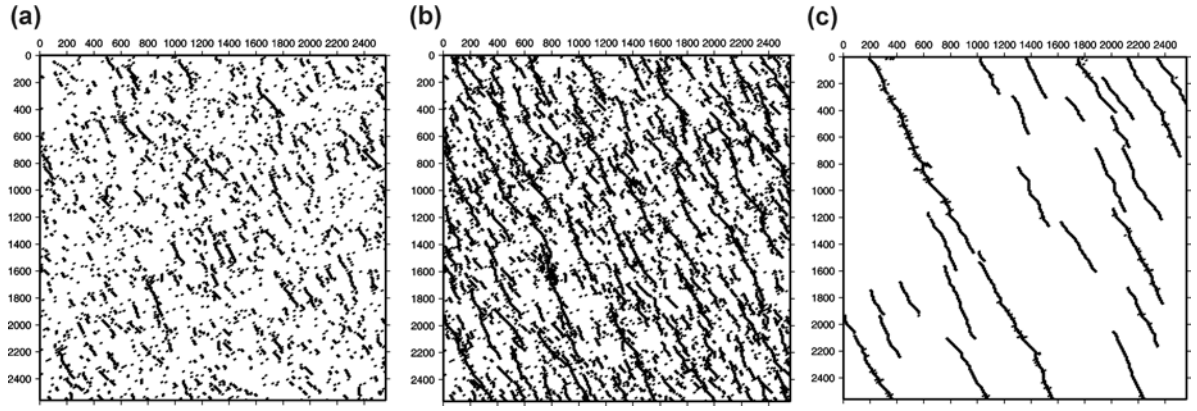

Fig. 1. Fault patterns that represent consecutive stages at the evolution of the fracturing. The horizontal direction is the x-direction (metres) and the vertical direction is the y-direction (metres). In figure (a) the pattern in represents the initial stages of the evolution, figure (b) shows a stage at which the system passed the percolation threshold, and figure (c) shows a later stage where the system is about to reach the quasi-steady state.

The background medium parameters are $V_P = 3300m/s$, $V_S = 2000m/s$, that are the P- and S-wave velocities, respectively, and the density is $\rho = 2200kgm^{-3}$. For the implementation of the fractures we assume that the fracture compliance's are constant having values $Z_T = Z_N = 5.6 \cdot 10^{-10} GPa^{-1}$. We use a grid of 256 x 256, with spatial grid-step $10m$ and time-step $0.001\sec$. The source wavelet is a Ricker wavelet with a dominant frequency of $30Hz$ and a pulse initial time of $0.1\sec$. The source is located in the center of the models $(x = 1280m, z = 1280m)$. For each medium we generate synthetic seismograms from where we calculate attenuation, and snapshots that exhibit the wave propagation at consecutive time steps. Figure 2 shows snapshots taken at 350ms after the initialization of the source for the fracture patterns (a), (b), and (c) respectively. From the snapshots we can see in Fig.2a a lot of scattered energy due to the high fracture density. In Fig.2b where the system is beyond the percolation threshold and the fracture density is much higher, the scattered energy is even higher, attenuation is significant and the wave front becomes ellipsoidal which indicates high anisotropy. Finally, in Fig.2c the system is close to the quasi-steady state and is reorganized into bigger fractures that result in reflected waves on the snapshots and less scattered energy compared with the previous stages.

Estimation of scattering attenuation

The estimation of Q requires a method that is robust and can handle the rapid spatial changes in the recorded waveform in such complicated media. We use the spectral method (McDonal et al., 1958), which calculates a Q estimate from the fit of a straight line to the spectral ratio of receiver and source power spectra recorded at different offsets from the source. It is assumed that the receivers lie along a common raypath from the source. Another assumption of the method is that the two power spectra can be linearly related by a simple attenuation operator. Deviations from a linear spectral ratio are treated as noise, and averaging of the spectra is usually required to give stable estimates of attenuation. The amplitude spectrum $A(\omega)$ of a wave after traveling a distance L in an attenuating medium is given by (Aki & Richards 1980)

$$A(\omega) = A_o(\omega) \exp\left[-\frac{\omega L}{2aQ(\omega)} \right], \tag{1}$$

where $A_o(\omega)$ is the amplitude spectrum of the source, a is the wave velocity, and $Q(\omega)$ is the attenuation factor of the medium. We replace $Q(\omega)$ by $Q_S(\omega)$, because in the numerical model

intrinsic attenuation is absent and the energy loss of the direct wave is caused by scattering only. We obtain for the scattering attenuation $Q_S^{-1}(\omega)$ as a function of frequency,

$$Q_S^{-1}(\omega) = -\frac{2a}{\omega L}\ln\left(\frac{A(\omega)}{A_o(\omega)}\right). \tag{2}$$

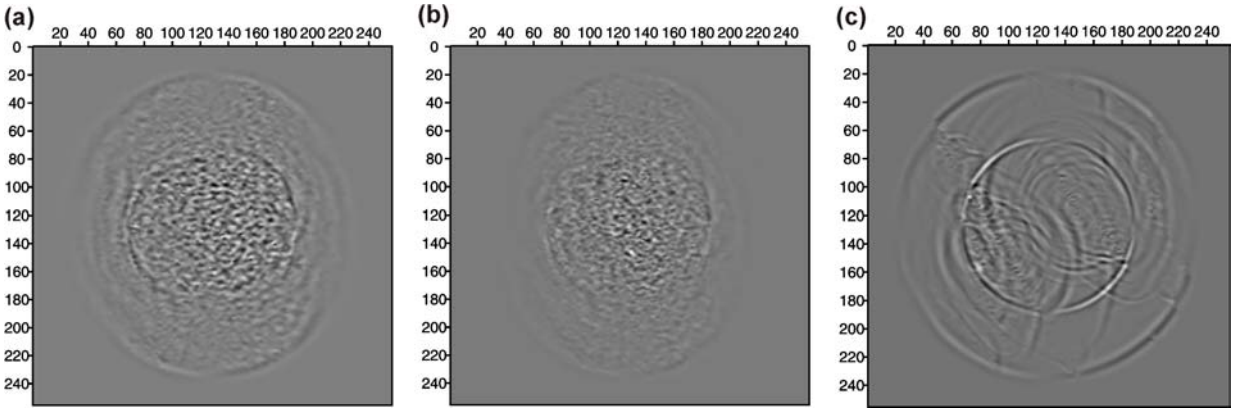

Fig. 2. Snapshots taken at 350ms after the initialization of the source. Figure (a), (b) and (c) correspond to the respective fault patterns of figure 1. The horizontal direction is the x-direction (x10 metres) and the vertical direction is the y-direction (x10 metres).

To calculate the amplitude spectrum $A(\omega)$ of the primary pulses, seismograms are windowed around the first arrival. The seismograms are Fourier transformed and the spectral ratio $A(\omega)/A_o(\omega)$ is computed. This ratio may in some cases yield negative values, corresponding to a magnification of the input signal caused by focusing effects of the heterogeneities. To calculate the scattering attenuation $Q_S^{-1}(\omega)$ we transform equation (2) into,

$$\ln\left(\frac{A(\omega)}{A_o(\omega)}\right) = -\frac{\omega Q_S^{-1}(\omega)}{2a}L. \tag{3}$$

We calculate for the receivers at different distances from the source the spectral ratios, and plot them as a function of distances. We fit a straight line to the values and from the slope of the line we calculate the scattering attenuation. That is for one frequency, and to calculate $Q_S^{-1}(\omega)$ for a range of frequencies we follow the same procedure for each frequency individually. $Q_S^{-1}(\omega)$ is evaluated in the frequency band 0 to 100 Hz.

Figure 3 shows the scattering attenuation values for the frequency range $(\omega = 0 - 628Hz)$ for the fault patterns presented in Fig.1. The results in very low and very high frequencies may not be accurate due to low energy content. Fig.3a corresponds to the fault pattern presented in Fig.1a. Scattering attenuation shows a rapid increase after 100Hz until it reaches its maximum value 251Hz. At that part we can say that it follows the characteristic behavior of Rayleigh scattering. Above this frequency attenuation drops constantly and has a local maximum at 447Hz. Figure 3b shows a different behavior of scattering attenuation. It starts from a higher value of attenuation compared to Fig.3a and constantly drops almost following a straight line, with an exception of a small change of trend around 263Hz. Finally, Fig.3c shows similar behavior with Fig.3a, starting from low values after 100Hz and constantly increasing until attenuation reaches its maximum value at 282Hz. In this case the increase is less sharp than in Fig.3a. After the maximum value it decreases steadily, once more following an almost straight line. In general, we have the highest values of attenuation in Fig.3b where we have the highest fracture density in the medium.

In terms of correlation with the statistical properties of the medium, there is indication that there are some links to the attenuation features. Figures 3a and 3c correspond to the medium at the initial stages of the formation and at the quasi-steady state, correspondingly. Both states will have some dominant

scale lengths of features, which interact with the energy traveling through the medium. In both figures there are certain frequencies where we have maxima or minima, and we believe they are linked with those characteristic length scales. On the other hand, Figure 3b that corresponds to a state above the percolation threshold does not show any maxima or minima, which we believe is due to the fact that above the percolation threshold there are no characteristic scale lengths. Thus, scattering attenuation can be a means of defining the state of the examined medium and possibly identifying characteristic scale lengths.

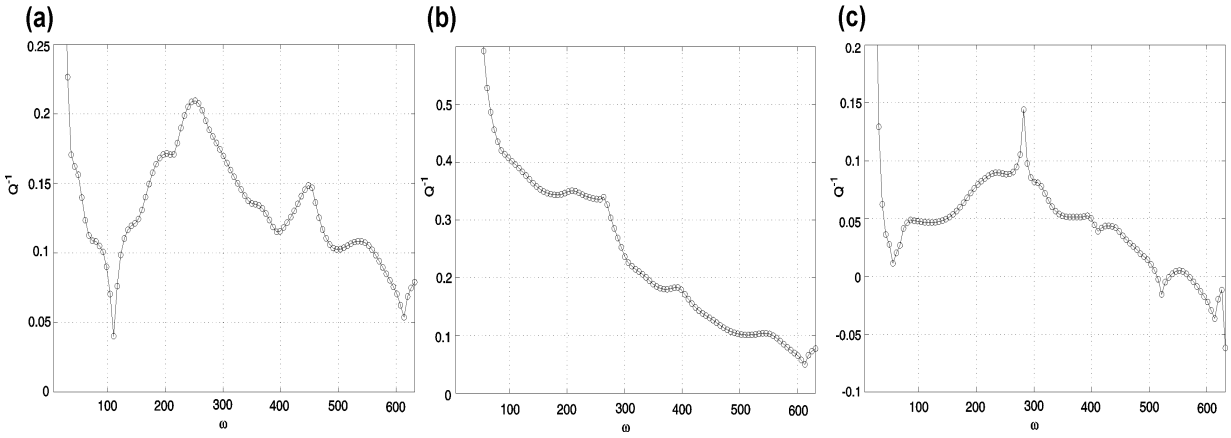

Fig. 3. Scattering attenuation as a function of frequency. Figures (a), (b) and (c), correspond to the mediums shown in Figure 1.

Conclusions

We have conducted a numerical study of scattering attenuation. We used a multiscale cellular automaton model to create three models of a fractured medium, which represent consecutive stages of the evolution of fracturing. We implemented a finite difference technique for forward modeling and generated synthetic seismograms and snapshots of the wave propagation in each of the models. To estimate the scattering attenuation as a function of frequency we used the spectral method. Our results indicate that there is a strong frequency dependence of scattering attenuation in all cases. We also believe that certain features of the attenuation, such as maximum or minimum values can be attributed to statistical properties of the media, ie. characteristic scale lengths of fractures. That indication becomes stronger by the lack of such features when the medium is in a stage that no characteristic scale length exists. Also we confirmed that a factor greatly affecting attenuation is fracture density, and that is why we have the highest attenuation when we have the highest fracture density. We believe that scattering attenuation can be a means of describing the properties of a medium, identifying dominant scale lengths, and can be used towards a more characterisation of a fractured reservoir.

Acknowledgements

This research is supported by the sponsors of the Edinburgh Anisotropy Project. This work is published with the approval of the Executive Director of the British Geological Survey and the EAP sponsors: BP, Chevron, CNPC, Conoco, DTI, ENI-Agip, Kerr-McGee, Landmark, Marathon, Norsk Hydro, PetroChina, PGS, Schlumberger, Texaco, TotalFinaElf, Trade Partners UK, and Veritas DGC. In the University of Edinburgh, Clement Narteau is supported through a Marie Curie fellowship No HPMFT-2000-00669 from the European Community.

References

Aki, K., and Richards, P.G., 1980, *Quantitative Seismology*, **vol.I, II**, Freeman, San Francisco.

McDonal, F.J., Angona, F.A., Mills, R.L., Sengbush, R.L., Van Nostrand, R.G., and White, J.E., 1958, Attenuation of shear and compressional waves in Pierre shale, *Geophysics*, **23**, 421-439.

Narteau, C., 2001, Formation and evolution of a population of strike-slip faults in a multiscale cellular automaton model, *Geophys. J. Int.*, in press.

Vlastos, S., Liu, E., Main, I.G., and Li, X.-Y., 2002, Numerical simulation of wave propagation in media with discrete distributions of fractures: effects of fracture sizes and spatial distributions, *Geophys. J. Int.*, in press.